Published in final edited form as:
Chem Res Toxicol. 2010 March 15; 23(3): 608–619. doi:10.1021/tx900351q.

IMMUNOSUPPRESSANT NEUROTOXICITY IN RAT BRAIN MODELS: OXIDATIVE STRESS AND CELLULAR METABOLISM

Jelena Klawitter[a,b,*,‡], **Sven Gottschalk**[b,c,‡], **Carsten Hainz**[b], **Dieter Leibfritz**[b], **Uwe Christians**[a], and **Natalie J. Serkova**[a,d]

Department of Anesthesiology, University of Colorado Denver, Aurora, Colorado, USA

[b]Department of Chemistry, Universität Bremen, Bremen, Germany

[c]Centre de Recherché, Centre Hospitalier de l'Université de Montréal, Hôspital Saint-Luc, Montreal, Quebec, Canada

[d]University of Colorado Cancer Center, University of Colorado Denver, Aurora, Colorado, USA

Abstract

Co-administration of the calcineurin inhibitor cyclosporine (CsA) and the mTOR inhibitors sirolimus (SRL) or everolimus (RAD) increases efficacy of immunosuppression after organ transplantation. Neurotoxicity of CsA is a major clinical problem. Our goal was to assess the effects of CsA, SRL and RAD on the brain cell metabolism.

The studies included the comparison of immunosuppressant-mediated effects on glucose metabolism, energy production and reactive oxygen species (ROS) formation in perfused rat brain slices, primary rat astrocytes and C6-glioma cells.

In brain slices and astrocytes, CsA inhibited Krebs cycle metabolism, while activating anaerobic glycolysis most likely to compensate for the inhibition of mitochondrial energy production. SRL and RAD inhibited cytosolic glycolysis, but did not cause changes in mitochondrial energy production. CsA+SRL inhibited Krebs cycle and glycolysis, thus reducing the ability of the cell to compensate for the negative effects of CsA on mitochondrial nucleoside triphosphate synthesis. In contrast to SRL at the concentrations tested, RAD reduced the CsA-induced ROS formation and antagonized CsA-induced effects on glucose and energy metabolism. Surprisingly, in C6 cells, SRL and RAD exposure resulted in high ROS concentrations without significant impairment of cell metabolism.

Our results suggested that SRL enhances CsA-induced ROS formation and negative metabolic effects in brain cells, while RAD seems to antagonize the CsA effects. However, the three models showed different metabolic responses when challenged with the study drugs. In contrast to SRL, RAD enhances ROS formation in C6 glioma cells, but has only minor effects on normal rat brain tissue.

Corresponding author: Jelena Klawitter, Ph.D., Clinical Research & Development, Department of Anesthesiology, University of Colorado Denver, Bioscience East, Suite 100, 1999 North Fitzsimons Parkway, Aurora, Colorado 80045-7503, Phone: +1 720 961 4483, Fax: +1 303 724 5662, Jelena.Klawitter@ucdenver.edu.
‡**Both authors contributed equally to this work**

The authors declare no competing financial interests.

SUPPORTING INFORMATION
This information is available free of charge via the Internet at http://pubs.acs.org/

Keywords

reactive oxygen species; brain metabolism; cyclosporine; sirolimus; everolimus; immunosuppressant; nuclear magnetic resonance spectroscopy (NMR)

1. INTRODUCTION

The cyclic undecapeptide cyclosporine (CsA) has been used as a baseline immunosuppressant after organ transplantation and in the treatment of autoimmune disorders for the last three decades (1,2). CsA exerts its immunosuppressive action by binding to cyclophilin and subsequent inhibition of calcineurin phosphatase activity (2). Calcineurin inhibition prevents dephosphorylation of the nuclear factor of activated T-lymphocytes (NFAT) and subsequently inhibits IL-2 synthesis and release, hence inhibiting T-lymphocyte proliferation (3). In addition to its major side effects nephrotoxicity, hyperlipidemia and diabetes, CsA exhibits neurotoxicity in transplant patients. Neurotoxicity is more frequently associated with high CsA blood concentrations, but also occurs during long-term treatment and CsA blood concentrations within the therapeutic target range (4–6). Clinical symptoms include tremor, severe headache, epileptic seizures, paraesthesia, cortical blindness and stroke (7,8). CsA is a well known inhibitor of the mitochondrial permeability transition pore (MPTP), which plays an important role in apoptosis induction, and, therefore, can be neuroprotective during hypoxia (9). In previous studies we have shown that CsA significantly decreased concentrations of high-energy phosphates such as phosphocreatine (PCr) and NTP in rat brain slices (10,11), as well as in the rat brain *in vivo* (12), by inhibiting brain energy metabolism including negative effects on Krebs cycle metabolism and mitochondrial oxidative phosphorylation.

The exact mechanisms underlying the negative effects of CsA on the brain are not yet fully understood, but the increase of oxidative stress in cells has been discussed in several reports. Wolf et al. (13) found a CsA-dependent increase in oxidative stress in primary rat hepatocytes and supplementation with ascorbic acid protected from CsA toxicity. Andrés et al. (14) described a difference in the induction of superoxide dismutase and catalase gene expression. The results suggested a CsA concentration-dependent imbalance in the cell defense systems against ROS. However, most of these studies have used high, clinically non-relevant CsA concentrations in the micromolar range. In transplant recipients CsA trough blood concentrations are maintained below 300 nM (equivalent to 360 μg/L)(1) and the associated maximum blood concentrations typically reach 900–1500 nM.

Since CsA has a narrow therapeutic index nowadays most immunosuppressive protocols include co-administration of other immunosuppressive agents that allow for reduction of CsA doses (15). This should reduce the incidence of CsA toxicity while maintaining immunosuppressive efficacy. The macrolides sirolimus (SRL) and its 40-O-(-2-hydroxyethyl) derivative everolimus (RAD) are attractive for co-administration with CsA due to their synergistic immunosuppressive activity and clinical studies have confirmed significantly decreased numbers of acute rejection episodes when CsA and SRL or RAD are combined (16,17). In lymphocytes, both macrolides inhibit the proliferation pathways via mTOR (mammalian target of rapamycin) (18). Clinical trials have reported increased nephrotoxicity during combination therapy of CsA and SRL in transplant recipients (19). This was a surprising observation, since in contrast to CsA both macrolides alone are neither nephrotoxic nor neurotoxic (20).

In our previous studies, we found that SRL and CsA interacted synergistically on the inhibition of energy production (10,12). In contrast, RAD antagonized CsA-related negative effects in rat brain energy state (12,21). As of to date, there is little information regarding the effects of

SRL and RAD on the ROS-balance. The CsA-induced increase of ROS was mainly analyzed in non-neuronal cells (13–15). Here we hypothesize that SRL and RAD modify CsA-induced ROS formation in neuronal cells and tissues.

In addition to the *ex vivo* brain slices, we included primary astrocytes and C6-glioma cells as *in vitro* monolayer cell models in our present study. Astrocytes are the most metabolically active cell type in the brain and function as protectors and detoxifying partners for neurons (22). They provide metabolic support for active neurons: by regulating blood flow to increase the availability of glucose and subsequently by taking up and trafficking glucose through a network of connecting astrocytes (23). Since functioning as a protective metabolic barrier for neurons and glial cells (23), we expected the astrocytes to mimic the metabolic profiles of immunosuppressant-treated brain slices. The C6 cell line has been widely used as a cell model for studies of glial cell development and differentiation (24,25).Because of the increased interest in targeting mTOR kinase signaling in anti-cancer therapy (26), use of C6 cells provided additional benefits not only as a model for studies of immunosuppressant toxicity on the glial brain cells but also for the investigation of the effects of mTOR inhibitors sirolimus and everolimus in cancerous cells versus normal brain.

Nuclear magnetic resonance spectroscopy (NMR) was developed as a principal method for evaluating molecular structure and conformation. More recently, it has increasingly been utilized as a non-invasive and non-destructive technique that can help physicians diagnose disease and detect early adverse effects of drugs. NMR-based metabonomics is defined as “the quantitative measurement of the time-related multiparametric metabolic response of living systems to pathophysiological stimuli or genetic modification” (27,28). Its is based on the fact that in most cases disease, drugs and toxins cause perturbations of the concentrations and fluxes of endogenous metabolites involved in key cellular pathways. Due to a wide range of metabolites screened by NMR and advanced data analysis techniques, drug toxicity profiles and mechanisms of action can be identified (29,30).

In this study, we used NMR-based metabolic profiling to test our hypothesis that SRL and RAD modify CsA-induced oxidative stress, by studying the effects of the study drugs on the formation of ROS, energy production and glucose metabolism. The changes in ROS production were measured using a fluorescence-based assay and were correlated with the changes in cell metabolism as evaluated by NMR. The secondary goal of the present study was to assess potential differences in the responses of the models tested during exposure to immunosuppressants under similar conditions.

2. EXPERIMENTAL PROCEDURES

2.1. Materials

CsA and SRL were purchased from Sigma (Munich, Germany) and RAD was kindly provided by Novartis Pharma AG (Basel, Switzerland). One mg/ml of CsA and 0.1 mg/ml of SRL and RAD were prepared in acetonitrile/water (80/20 vol/vol) as stock solutions. The perfusion medium for rat brain slices was standard Krebs Balanced Salts (BSS) containing 100 mM NaCl; 0.1 mM KH_2PO_4; 6.1 mM KCl; 5 mM glucose; 24 mM $NaHCO_3$; 1.2 mM $CaCl_2$ (anhydrous); 1.2 mM $MgSO_4 \cdot 7H_2O$ and 25 mM HEPES (pH 7.4). For ^{13}C-NMR experiments 5 mM [1-^{13}C]-labeled glucose (Cambridge Isotope Laboratories, Andover, MA) was used instead of unlabeled glucose.

The fluorescence probe 2′,7′-dichlorofluorescin diacetate (DCFH-dAc) was from Molecular Probes Europe (Eugene, NL). A stock solution of 20 mM in ethanol was prepared and stored at −20°C. Incubation of cells with the fluorescence probe and fluorescence measurements of cells and brain slices were carried out in a so-called measurement buffer containing 5 mM

glucose; 1 mM $MgCl_2$; 1 mM NaH_2PO_4; 1.3 mM $CaCl_2$; 120 mM NaCl; 25 mM HEPES; 5.4 mM KCl; pH 7.35.

Rat C6-glioma cells were purchased from ICN Biomedicals (Meckenheim, Germany). Dulbecco´s Modified Eagle Medium (DMEM), fetal calf serum (FCS), penicillin/ streptomycin, phosphate buffered saline (PBS) and trypsin were purchased from Gibco (Eggenstein, Germany). Tissue culture flasks and culture Petri dishes were from Nunc (Wiesbaden, Germany). Trimethylsilylpropionic-2,2,3,3-d4-acid (TSP) from Aldrich (Steinheim, Germany) and deuterated solvents as well as ethylenediaminetetraacetic acid (EDTA) were from E. Merck (Darmstadt, Germany).

2.2. Preparation of rat brain slices

All animal protocols were reviewed and approved by the Universität Bremen Committee on Animal Research. Six 8-day-old Wistar rats (Charles River, Sulzfeld, Germany) were used per experiment. Twelve cerebrocortical slices (~350 μm thick) were prepared as described previously (11) and perfused with Krebs BSS under 95% oxygen/5% CO_2 at 37°C. Two hours after slice preparation, allowing for metabolic recovery, brain slices were perfused after addition of drug-free vehicle (negative controls), H_2O_2 (positive controls), CsA, SRL, RAD, CsA+SRL, or CsA+RAD. Three slices were used for fluorescence measurements and nine for NMR-based metabolic profiling.

2.3. Cell culture conditions and primary astrocytes preparation

C6-glioma cells and primary astrocytes are both adherently growing cells. The cultures were incubated at 37°C with 10% CO_2 in atmospheric air. The growth medium used was DMEM and cells were grown to confluence prior to experiments in 10- or 15-cm Petri dishes for fluorescence or NMR studies, respectively. C6-glioma cells were incubated with medium containing 5% FCS and primary astrocytes with medium containing 10% inactivated FCS.

Primary astrocytes were prepared from brains of 2-day-old newborn rats following the procedures described by Booher and Sensenbrenner (31). Briefly: the cerebral hemispheres were dissected from the brains, the meninges were cut out and the cerebral tissue was mechanically disrupted and centrifuged. The resuspended cell pellets were plated on 260 mL culture flask (one brain/flask) containing 20 mL medium. To remove other glia cells, the medium was completely exchanged 24 hours after seeding. During the next three days the flasks were not moved. Seven days after preparation the cells were removed from the culture flasks by mild trypsinization (500 mg/L trypsin and 20 mg/L EDTA) and replated in 10 cm culture Petri dishes (6 per flask) for oxidative stress measurements or in 15 cm culture Petri dishes (3 per flask) for NMR studies. The cultures were allowed to grow for another 14 to 20 days until confluency was reached. The growth medium was changed 2–3 times per week.

2.4. Drug treatment

Seven study groups were assigned: 1) untreated control with drug-free vehicle; 2) 500 μg/L CsA; 3) 100 μg/L SRL; 4) 100 μg/L RAD; 5) 500 μg/L CsA + 100 μg/L SRL; 6) 500 μg/L CsA + 100 μg/L RAD and 7) positive control for oxidative stress with H_2O_2 (0.1 mM for C6-glioma cells and primary astrocytes and 1mM H_2O_2 for rat brain slices). The concentrations of the immunosuppressants were chosen based on our previous, systematic dose finding studies (10) and are close to the concentration range typically found in blood in transplant patients (cyclosporine: 80–200 (C_{12h})- 1500 ng/mL (= C_{max}) and sirolimus: 3–15 ng/mL (C_{24h}) – 30–100 ng/mL (C_{max})). The concentrations chosen were the minimum concentrations that resulted in a detectable change in cell metabolite patterns in our previous studies (10). The total incubation time with immunosuppressants was 3 hours, the incubation time with H_2O_2 was 30 minutes. For ^{13}C-NMR studies [1-^{13}C]glucose (5 mM) instead of unlabeled glucose was used

for the 3 hours of incubation. The incubation time of 3 hours used in the present study was based on the study (32) and is a time close to the maximum negative effect before compensatory mechanisms start to partially compensate for some of the drug effects on cell metabolism.

2.5. Oxidative stress measurements

DCFH-dAc (2´,7´-dichlorofluorescin diacetate) is cleaved intracellular by esterases to its non-fluorescent form 2´,7´-dichlorofluorescin (DCFH) and then oxidized to highly fluorescent 2', 7'-dichlorofluorescein (DCF) (33).

2.5.1. Brain slices—After 2 hours of perfusion (first 30 minutes at 25°C, rest of the time at 37°C) in EBBS buffer containing 5 mM glucose to allow for metabolic recovery, the perfusion-buffer was changed and the study drugs were added. Perfusion was continued for another 3 hours and the fluorescent probe DCFH-dAc (50 μM) was added to the buffer for the last hour of perfusion. In study group 7) 1mM H_2O_2 as a positive oxidative stress control was added for the last 30 min of perfusion. Afterwards the brain slices were washed with ice-cold PBS, weighed and homogenized in 5 mL of measurement buffer.

2.5.2. Cells—After 3 hours of incubation with the immunosuppressants or 30 minutes with 0.1 mM H_2O_2, the medium was removed, the cells were washed with PBS buffer, trypsinated, collected in 2 mL Eppendorf vials, centrifuged and redissolved in 2 mL of measurement buffer. Study drugs and 50 μM DCFH-dA were added. After incubation for 30 minutes at 37°C in the dark the cells were centrifuged and resuspended in 1 mL of measurement buffer. An aliquot was stored at –20°C for protein determination.

Fluorescence was measured with a Perkin-Elmer LS50B fluorescence spectrometer (excitation wavelength: 485 nm, emission wavelength: 525 nm) for 3 min. Homogenates of brain slices has been diluted 1:10 in measurement buffer prior to recording fluorescence. After 90 seconds, H_2O_2 was added at a concentration of 0.25 mM to verify the loading of the cells with the fluorescence probe.

2.6. Perchloric acid (PCA) extraction of rat brain tissue and cells for NMR analysis

2.6.1. Brain slices—After 3 hours of treatment in the presence of [1-^{13}C]glucose (the incubation with H_2O_2 was carried out during the last 30 minutes before extraction), brain slices were washed with ice-cold PBS and immediately frozen in liquid nitrogen. Nine frozen brain slices were weighed, pulverized in the presence of liquid nitrogen and extracted with 4 mL of ice-cold 12% PCA (11,12). After centrifugation at 1300g for 10 minutes at 4°C the aqueous phase was collected, neutralized with KOH, centrifuged again to remove potassium perchlorate and lyophilized overnight.

2.6.2. Cells—After 3 hours of incubation with 5mM [1-^{13}C]glucose and study drugs (the incubation with H_2O_2 was carried out during the last 30 minutes before extraction), the cells were washed with 0.9% isotonic ice-cold NaCl-solution and immediately frozen in liquid nitrogen. The frozen cells were harvested using 2 mL ice-cold 12% PCA followed by 2 mL H_2O. For each treatment group four confluently grown 15 cm-Petri dishes were used. The extracts were centrifuged at 1300 g at 4°C for 10 minutes. The supernatant was lyophilized overnight. All lyophilized PCA-extracts were redissolved in 0.5 mL deuterium oxide (D_2O) and the pH was adjusted to 7.0 using DCl and NaOD prior to NMR-measurements. After centrifugation, the supernatants were analyzed by NMR.

2.7. NMR

All one-dimensional NMR-spectra of tissue and cell extracts were recorded using an AMX 360 MHz spectrometer (equipped with a 5mm-QNP probe, Bruker, Karlsruhe, Germany).

Proton, carbon-13 and phosphorous-31 spectra were zero-filled and Fourier-transformed, phase-and baseline corrected and signal integrals were measured using the 1D–XWIN-NMR software (Bruker, Karlsruhe, Germany). For ^{1}H spectra line broadening of 0.1 Hz, for ^{13}C and ^{31}P spectra 1.0 Hz were used.

2.7.1. ^{1}H-NMR—For ^{1}H-NMR analysis of water-soluble extracts we used fully relaxed spectra with a standard water presaturation pulse program. Spectra were obtained at 12 ppm spectral width, 32K data arrays, and 64 scans with 90-degree pulses applied every 14.8 sec. The pool size of metabolites was determined based on fully relaxed ^{1}H-NMR spectra of extracts using trimethylsilyl propionic-2,2,3,3,-d_4 acid (TSP, 0.6 mmol/l for water-soluble extracts) as an external standard and chemical shift reference (0 ppm). The absolute concentrations of each metabolite [metabolite] were determined and normalized according to cell wet weight, as previously described (34–36) and calculated using the following equation:

$$[\text{metabolite}]=\{\text{integral}_{\text{met}} \times [\text{TSP}] \times V_S\} / [\text{integral}_{\text{TSP}} {}^{*}\text{wet weight}]$$

whereas integral$_{met}$: integral of respective metabolite signal divided by the number of protons; integral$_{TSP}$: integral of TSP signal divided by the number of protons; [TSP]: TSP nominal concentration; V_S: sample volume; wet weight: sample weight.

2.7.2. ^{13}C-NMR—^{13}C-NMR spectra with proton decoupling (composite pulse decoupling (CPD)) were recorded using the C3-lactate peak at 21 ppm as chemical shift reference (spectral width was 150 ppm, 16K data arrays, with 20K scans applied every 3 sec). For quantification of absolute concentrations of ^{13}C metabolites, calculations were made according to (37,38). The ^{13}C-enrichments in C3-lactate were determined by the heteronuclear spin-coupling pattern in ^{1}H-NMR spectra as follows:

$$^{13}\text{C}-\text{enrichment}=[\text{area}\,(^{1}\text{H}-{}^{13}\text{C}) \times 100]/[\text{area}\,(^{1}\text{H}-{}^{12}\text{C})+\text{area}\,(^{1}\text{H}-{}^{13}\text{C})]$$

whereas the sum (area [^{1}H-^{12}C] + area [^{1}H-^{13}C]) is equivalent to the pool size of lactate. The values were corrected for the 1.1% natural abundance of ^{13}C. ^{13}C-enrichments in individual carbons of amino acids were derived from ^{13}C-NMR spectra using the known ^{13}C-enrichment in lactate:

$$E_{\text{Met}}(\%)=[A_{\text{Met}} - A_{\text{n.a.}}(\text{Met})] / A_{\text{n.a.}}(\text{Met})] \times 1.1$$

whereas A_{Met} represents ^{13}C carbon peak area of the metabolite, $A_{n.a.}$ its natural abundance signal intensity, and 1.1 is the percentage factor of the ^{13}C-isotope. The natural abundance of ^{13}C, contributing to the total intensity $A_{n.a.}$(Met), was determined using the known ^{13}C-enrichment and natural abundance of lactate and correction for the pool size:

$$A_{\text{n.a.}}(\text{Met}) = \{A_{\text{Lac}} \times [\text{Met}]\}/\{(E_{\text{Lac}}+1) \times [\text{Lac}]\}$$

A_{Lac} represents the carbon peak area of lactate, [Lac] or [Met] the pool sizes of lactate or metabolite of interest, respectively, and E_{Lac} the percentage ^{13}C-enrichment in lactate.

The ^{13}C signal intensities were corrected for nuclear Overhauser enhancement (NOE) effects by comparison with a standard mixture of amino acids.

The absolute amount of ^{13}C in specified carbon positions is the product of the pool size times the fraction of ^{13}C-enrichment.

The absolute amount of ^{13}C in specified carbon positions is the product of the pool size times the fractional ^{13}C-enrichment.

2.7.3. ^{31}P-NMR—Before ^{31}P-NMR analysis EDTA was added to the same PCA extract to complex divalent ions 100 mM. This resulted in ^{31}P spectra with significantly narrower line width. The pH was adjusted to 7.0 using NaOH and HCl. Spectra were obtained at 20 ppm spectral width, 8K data arrays, and 5K scans with 84-degree pulses applied every 4 sec. Phosphocreatine (PCr) was used as a chemical shift reference at −2.33 ppm. Also, concentrations of PCr (as calculated from the ^{1}H-NMR spectra in nmol/g wet weight) served as internal standard for phosphorous metabolite quantification.

2.8. Protein determination

An aliquot of the cell suspensions from the fluorescence measurements was used in a modified Biuret reaction as described by Goa (39). Cell suspensions were centrifuged and the cell pellet was re-suspended in 0.015 M KOH. Reaction with the Biuret reagent solution was carried out in a 96-multiwell-plate with appropriate dilutions. Absorption was measured at 540 nm after 40 minutes. The protein concentrations were calculated using bovine serum albumin as standard.

2.9. Statistical analysis

All numerical data are presented as means ± standard deviations from replicate experiments. One-way analysis of variance (ANOVA) was used to test for differences among groups. Tukey's test was used as a *post-hoc* test in combination with ANOVA to test for significances levels between groups. The significance level was set to $p<0.05$ for all tests (SigmaPlot-version 11.0, Systat Software, Point Richmond, CA and SPSS version 17.0, SPSS Inc., Chicago, IL).

3. RESULTS

Figure 1 shows an example of fluorescence recordings in treated homogenized brain slices. Addition of H_2O_2 was used to verify loading of the cells with DCFH-dA. The increase in fluorescence intensity is proportional to the angle α and correlates with the production of ROS in the cells and tissues. Hence an increase in fluorescence provides evidence for an imbalance of ROS-production and degradation.

3.1. ROS after immunosuppressive treatment

3.1.1. Brain slices—After 3 hours of incubation, all immunosuppressants caused an enhanced production of ROS as indicated by an increase of fluorescence intensity (Figure 2A). One-way ANOVA with Tukey *post-hoc* test was performed to assess potential statistically significant changes among and between groups. None of the treatments reached the level obtained with H_2O_2 (increase in DCF-fluorescence per gram wet weight 0.20±0.06, n=6, *versus*. 0.05±0.03 in the controls, n=5, $p<0.001$). CsA, SRL and the combination of CsA+SRL produced high levels of ROS as well (Figure 2A). RAD itself was not significantly different from other treatment groups (except for H_2O_2), but its combination with CsA showed a significantly lower ROS level compared to CsA+SRL combination treatment ($p<0.05$, n=5).

3.1.2. Astrocytes—None of the treatments with immunosuppressants induced statistically significant changes in the ROS production in rat primary astrocytes compared to controls (Figure 2B). The highest ROS levels were observed with H_2O_2 and CsA+SRL treated astrocytes (increase in DCF-fluorescence per gram protein to 13.51±4.13 and 10.90±1.05, n=3). The only significant difference was observed in the CsA+SRL group, where the addition of CsA augmented the ROS production (SRL *versus* CsA+SRL, $p<0.05$, n=5).

3.1.3. C6-glioma cells—The baseline ROS-level in the untreated C6-glioma cells was lower than in primary astrocytes (DCF-fluorescence per gram protein: 2.25±1.48 *versus*. 6.99±2.59, Figure 2B). The glioma-cell line was most sensitive when treated with the two anti-proliferative mTOR inhibitors SRL and RAD, exhibiting a three- to four-fold increase in ROS production (SRL: 18.94±4.71, n=6, $p<0.0001$versus controls, RAD: 18.86±4.32, n=6, $p<0.0001$ versus controls). The CsA and combination groups showed only a slight increase in the ROS levels (Figure 2B). One-way ANOVA with Tukey's *post-hoc* test showed that SRL and RAD ROS levels were significantly higher then in all other treatment groups, including positive and negative controls.

3.2. Metabolic response to immunosuppressant-induced oxidative stress as evaluated by NMR

^{1}H- and ^{31}P-NMR allow for simultaneous identification and quantification of a large number of endogenous metabolites (Figure 3), while addition of ^{13}C-glucose allows for calculations of metabolic fluxes within the cell (Figure 4). Since glucose is the main energy substrate in the brain, we studied the effects of CsA, SRL and RAD alone, and in combination on glucose metabolism using 5 mM [1-^{13}C]glucose and *ex vivo* ^{13}C-NMR analysis of rat brain models. This allowed for detection of ^{13}C-labeled glucose-metabolism intermediates in the ^{13}C-NMR-spectra such as ^{13}C-labeled Krebs cycle intermediates (C2, C3, C4-glutamate and glutamine; C2-, C3-aspartate, C2-succinate) and ^{13}C-labeled glycolysis intermediates (C3-lactate; C3-alanine). The ratio between Krebs cycle and glycolysis intermediates was used as an indicator for the balance between oxidative and anaerobic metabolic pathways (Table 1, Figure 4)). The changes in high-energy phosphates are shown in Table 2 and Figure 3B.

3.2.1. Brain slices—Addition of H_2O_2 to the perfusion medium led to a decrease of ^{13}C-labeled Krebs cycle intermediates. The concentrations of [4-^{13}C]-labeled glutamate was significantly reduced by H_2O_2 (as compared to controls, Table 1). In comparison, brain slices treated with CsA alone and in its combination with SRL gave similar results (Table 1). Both groups showed a decrease of the C4-glutamate signal (Table 1) and, interestingly, were significantly lower than in the brain slices exposed to SRL alone (one-way ANOVA Tukey post-hoc $p<0.05$, CsA or CsA+SRL versus SRL). In addition, the CsA+SRL treatment group revealed a significant reduction of the C3- and C4-glutamine signals to 40.4% (n=4, $p<0.05$) and 61.6% of the controls (n=4, $p<0.01$). Only the H_2O_2 treated group showed a greater reduction (decreased to 18.6% (n=4, $p<0.05$) and 32.8% of the controls (n=4, $p<0.005$, respectively).

In regards to glycolysis, treatment with RAD, SRL or the combination of CsA+SRL caused a significant decrease the C3-lactate concentrations as did the treatment with H_2O_2 (Table 1). CsA alone significantly increased C3-lactate production (127.5% of control, n=4, $p<0.05$) and also reversed the C3-lactate lowering effect of RAD when combined (no significant change *versus* the controls, Table 1; with one-way ANOVA in combination with Tukey's *post-hoc* test $p<0.05$ for CsA+RAD *versus* RAD). On the other hand, addition of SRL to CsA markedly decreased C3-lactate concentrations (C3-lactate: 57.9% of the controls, n=4, $p<0.005$). This reduction was statistically significant when compared to brain slices exposed to CsA alone

($p<0.0001$) as well as to CsA+RAD ($p<0.05$, ANOVA in combination with Tukey's *post hoc* test).

Since the brain's energy production is highly dependent on glucose metabolism, it was not surprising that the three groups which showed a decrease in Krebs cycle fluxes (H_2O_2, CsA and CsA+SRL) also demonstrated the biggest decline in the cells' energy balance (NTP/NDP ratio, Table 2, Figure 3B) and a reduction of NAD(H) concentrations (Table 2, Figure 3B). Furthermore, the concentration of the high energy phosphate phosphocreatine (PCr, Table 2, Figure 3B) was diminished after H_2O_2, CsA, SRL and CsA+SRL treatments. SRL alone only slightly decreased PCr and NTP concentrations without any effect on NAD(H). RAD, in contrast, greatly increased NAD(H) concentrations (182.8% of control, n=4, $p<0.005$, Table 2), indicating an induction of mitochondrial energy production, with a subsequent increase of PCr concentrations (125.3% of control, n=4, $p<0.05$, Table 2). In combination, CsA+SRL markedly decreased the NTP/NDP ratio as well as PCr and NAD(H) concentrations (Table 2, Figure 3B). After exposure to CsA+SRL, PCr concentrations and NTP/NDP-ratios were significantly lower than in all other immunosuppressant groups ($p<0.05$), whereas the NAD (H) concentrations were lower than after RAD and CsA+RAD treatments (one-way ANOVA with Tukey's *post-hoc* test, $p<0.05$). This went parallel with an inhibition of the Krebs cycle and glycolytic fluxes as described above. Once again, the concentration changes of energy substrates in the CsA+SRL groups were similar to those after H_2O_2 treatment. CsA+RAD-treated brain slices showed only a slight decrease in high energy phosphate concentrations (significantly less than CsA alone, $p<0.01$). In combination, RAD antagonized CsA-induced reduction in NAD(H) concentrations (Table 2, Figure 3B).

Compared to the controls. concentrations of the neuronal marker N-acetyl-aspartate and the neurotransmitter γ-aminobutyric acid (GABA) were not changed in SRL, RAD and CsA+RAD treatment groups (Figure 3A and Figure 5A). However, their concentrations were decreased in the presence of CsA and CsA+SRL, and were significantly lower than in brain slices treated with RAD or CSA+RAD (Tukey's *post-hoc* test, $p<0.05$, Figure 5A). Exposure of brain slices to CsA+SRL also resulted in a significant decrease of myo-inositol, an osmoregulator (Figure 3A and Figure 5A).

3.2.2. Astrocytes—CsA-treated primary astrocytes showed changes of metabolite patterns similar to those observed in isolated brain slices. The concentrations of ^{13}C-labeled Krebs cycle intermediates such as C4-glutamate were decreased (Table 1) and glycolysis rates were enhanced as indicated by increased C3-lactate formation (Table 1). These changes went parallel with a reduced Krebs cycle/glycolysis ratio as observed in CsA-treated brain slices. When combined with SRL, CsA-mediated inhibition of Krebs cycle was enhanced (C4-glutamate concentration, $p<0.05$, Table 1) while SRL reversed the CsA-mediated increase of glycolysis (C3-lactate concentration, $p<0.05$ for CsA+SRL *versus* CsA, Table 1). SRL alone significantly reduced C3-lactate production indicating inhibition of anaerobic glycolysis. RAD alone, as well as in the combination with CsA, did not change the metabolite fluxes in neither the Krebs cycle nor the glycolysis in primary astrocytes.

After exposure to CsA, PCr concentrations and the NTP/NDP ratios were lower than in the negative controls (Table 2). Again, like in the brain slices, CsA+SRL not only inhibited the production of labeled Krebs cycle and glycolysis intermediates but also markedly decreased the energy balance ([NTP/NDP]: 1.81 versus 3.47 in the controls, Table 2) with greatly decreased NTP, PCr and NAD(H) concentrations. Only incubation with H_2O_2 resulted in an even greater reduction of high energy phosphates and NAD(H) concentrations (Table 2).

The concentration of the so-called fast volume regulator myo-inositol was slightly decreased in astrocytes treated with CsA (71.7% of the controls, $p<0.05$), CsA+SRL (76.2% of the

controls, $p<0.05$) as well as with H_2O_2 (55.4% of the controls, $p<0.001$) (Figure 5B), indicating astrocytes swelling. Treatment with H_2O_2 also caused a decrease of the so-called slow volume regulators, hypotaurine and taurine (Figure 5B), an effect that was also seen only with the combination of CsA+SRL, albeit to a lesser extent.

3.2.3. C6-glioma cells—In the cancer C6 cell line, a significant decrease of *de novo* synthesized lactate concentrations was observed after their exposure to SRL and RAD with no additional effect when CsA was added (Table 1, Figure 4).

In regards to the effects of the immunosuppressants on mitochondria, CsA decreased C4-glutamate to a lesser extent than the mTOR-inhibitors and even slightly increased the C4-glutamate concentration when combined with SRL or RAD (Table 1, Figure 4). All immunosuppressants significantly decreased the production of C3-lactate (Table 1). Their effects were comparable to those of H_2O_2 in regards to the decrease of metabolic fluxes within the Krebs cycle and glycolysis (Table 1, Figure 4). However, the accumulation of intracellular glucose was observed only in SRL-treated cells (5060 nmol/g in SRL *versus* 3327 nmol/g in the controls ($n=4$, $p<0.05$) and *versus* 4590 nmol/g in CsA+SRL ($n=4$, $p<0.05$) (Table 1).

As found in rat brain slices and primary astrocytes, C6-glioma cells also showed a significant decrease in the energy balance under all treatment conditions (Table 2). At the same time the concentrations of the short-term energy reservoir PCr significantly declined in all treatment groups except after exposure to CsA alone (Table 2). The concentrations of NAD(H), was also significantly reduced in all groups and but most markedly after exposure to CsA+SRL, CsA +RAD and H_2O_2 with the negative effects more pronounced in this order (Table 2). In fast proliferating C6-glioma cells, the immunosuppressants greatly affected the concentrations of phosphocholine (PC) with concentrations reduced to 25% and less of those in the controls (420.7±169.3 nmol/g weight in controls; 83.5±12.8 nmol/g weight after H_2O_2; 58.5±38.9 nmol/g weight after SRL; 100.3±70.1 nmol/g weight after CsA+RAD exposure; all $n=3$, $p<0.005$).

A decrease in the concentrations of myo-inositol and taurine, the main volume regulators of brain cells, was observed after treatment with CsA and H_2O_2 (and taurine in case of CsA+SRL), again most likely indicating cell swelling (Figure 5C).

4. DISCUSSION

NMR-based metabolic profiling approaches allow for the simultaneous assessment of a multitude of important cellular metabolic pathways including glucose, high-energy phosphate and lipid metabolism (27) and are a valuable tool in the evaluation of unknown toxicodynamic mechanisms. In our study we took advantage of non-invasive *ex vivo* and *in vitro* NMR to study effects of immunosuppressants and correlate those with the production of free radicals, widely accepted mediators of tissue injury in several neurodegenerative states (40,41).

The goal of the present study was to test our hypothesis that SRL and RAD modify CsA-induced ROS formation in neuronal cells and tissues and to evaluate the related effects on neuronal cell metabolism.

Three different established neuronal cell models were chosen to reduce model-dependent effects and to increase the robustness of the conclusion: perfused rat brain slices as an *ex vivo* brain model, rat primary astrocytes and C6-glioma cells as *in vitro* models.

While the mechanisms of CsA immunosuppressive action are well understood, only little is known about the biochemical mechanisms underlying CsA-toxicity (42). Our studies in brain slices showed that exposure to the immunosuppressants tested alone and in combination

resulted in significant ROS-production. Since brain slices represent an *ex vivo* model while preserving the brain cell structure and cell interactions, they are probably the model among the three models included in the present study that gives the most valid data in terms of translation into the *in vivo* situation.

It is well known that free radicals react with membrane lipids, cellular proteins and nucleic acids and have a negative impact on cellular pathways such as the Krebs-cycle and mitochondrial oxidative phosphorylation (43). Most of these metabolic effects were found in our NMR studies and it seems reasonable to assume that these were driven by oxygen radicals. This is supported by our previous studies that showed that the oxygen radical scavenger vitamin E can completely reverse the negative effects of cyclosporine on mitochondrial oxidative phosphorylation in perfused brain slices (32).

Our results showed that CsA significantly reduced glucose metabolism *via* interference with the Krebs cycle, resulting in decreased concentrations of all Krebs cycle intermediates. Among the intermediates measured, concentrations of C4-glutamate were affected the most. CsA negatively affected mitochondrial oxidative phosphorylation, as was demonstrated by decreased NTP/NDP ratios. In addition, CsA treatment resulted in decreased NAA and GABA concentrations. NAA is a well-known putative marker of neuronal and axonal density (44, 45) and a measure of neuronal viability and function (46,47). Its reduction suggested CsA-induced loss of neuronal viability and function and/or a reduction in a number of neurons. Decline of GABA concentration as seen in case of CsA single and CsA combination treatment with SRL supports previous findings, which showed that CsA inhibited GABAergic neural activity and binding properties of the GABA receptor (48,49) and that these events are closely related to the occurrence of neurotoxic effects under CsA therapy.

Surprisingly, perfused brain slices and isolated primary astrocytes as non-cancerous models were more sensitive to CsA's negative metabolic effects than the C6-glioma cell line. A derailment of the mitochondrial oxidative phosphorylation most probably leads to an increased production of ROS. It is reasonable to expect that this results in a vicious cycle. ROS negatively affect mitochondrial oxidative phosphorylation resulting in formation of even more ROS (50). Our studies with H_2O_2 showed similar metabolic changes in glucose and high-energy phosphate metabolism as seen after incubation with CsA, indicating that the formation of ROS may be responsible for the extent of reduction in high-energy phosphates by CsA. A similar observation has been made in regards to the observed decline in the NAD(H)-concentrations after exposure to CsA or H_2O_2.

The CsA-mediated reduction of mitochondrial energy metabolism was compensated by increased cytosolic anaerobic glycolysis resulting in increased lactate concentrations. The decrease in the volume- and osmoregulator-concentrations after CsA mono- and combination-treatment with SRL is associated with cell swelling (51). Our studies, evaluating the effect of CsA on rat brain slices under normoxic and hypoxic conditions, suggested that the negative effects of CsA during normoxia and the protective effects during hypoxia were both due to reduction of the Ca^{2+}-efflux from mitochondria (51). Calcium overload of mitochondria may be an explanation for the inhibition of the Krebs-cycle and the reduction of high-energy phosphate metabolism by CsA found in our study. Based on the results of or previous studies evaluating the effects of CsA on brain metabolism, we proposed the following chain of events: CsA causes mitochondrial Ca^{2+} overload and leads to derailment of the oxidative chain and increased oxygen radical production.

To identify the mechanisms underlying the synergistic reduction of high-energy phosphates after treatment with CsA and SRL it is important to understand the basic molecular mechanisms of CsA-toxicity. Our results indicated that SRL did not directly affect mitochondrial energy

production. However, as indicated by our studies with ^{13}C-labeled glucose, SRL inhibited cytosolic anaerobic glycolysis, hence reducing the amount of pyruvate available for the Krebs-cycle and thus indirectly decreasing oxidative phosphorylation. The inhibition of glycolysis can be explained through the fact that sirolimus as an mTOR kinase inhibitor also inhibits the phosphorylation of AKT kinase and hence suppresses glycolysis (52,53). In combination, SRL enhanced the ability of CsA to reduce mitochondrial Krebs cycle and oxidative phosphorylation and prevailed in reducing C3-lactate concentrations as a product of anaerobic glycolysis. In addition, SRL and its combination with CsA had the greatest negative effect on neuronal viability as indicated by low levels of NAA in perfused brain slices and produced the highest levels of ROS.

Similar to SRL, RAD alone had no detectable direct effects on metabolic pathways in the mitochondria. But when combined with CsA, in contrast to the CsA+SRL combination, RAD antagonized CsA-induced reduction of high-energy phosphates and increased oxidative stress. The major reason for the difference between RAD and SRL is that RAD, in contrast to SRL, penetrates the mitochondrial membrane (54). However, the exact molecular mechanism of this antagonism remains to be evaluated.

In addition to the *ex vivo* brain slices, we have used primary astrocytes and C6-glioma cells as *in vitro* monolayer cell models. Because of their role as protective metabolic barrier for neurons and glial cells (23), we expected and confirmed that the astrocytes exhibit similar metabolic responses as brain slices exposed to the study drugs and their combinations. Interestingly, a recent publication identified astrocytes as the brain cells most sensitive to H_2O_2 toxicity (55). Therefore we decided to use lower concentrations of H_2O_2 in the cell cultures (astrocytes and glioma cells) than used for the brain slices.

In recent years, mTOR has been recognized as target in the therapy of human malignancies (56). SRL and RAD are known to inhibit mTOR (57). The potential of SRL and RAD as anti-cancer drugs and their effect on glioma cell proliferation has been recognized by other groups (58). In the C6-glioma cell line, both mTOR inhibitors SRL and RAD strongly induced ROS production.

Cancer cells are highly dependent on aerobic glycolysis to compensate for their high demands of ATP due to their increased proliferation rates (Warburg-effect) (59). While in C6 glioma cells CsA mainly affected the cytosolic glycolysis, both anti-proliferative mTOR inhibitors SRL and RAD affected the glycolysis as well as the mitochondrial metabolism, and therefore induced a more pronounced decrease in energy production in C6-glioma cells.

Interestingly, while the combination of CsA+RAD did not negatively affect either brain slices or primary astrocytes, it clearly showed a high impact on proliferation and metabolism of C6 glioma cells. Based on our results, it can be speculated that RAD may be an effective anti-cancer treatment with less negative effects on the normal brain cells compared to SRL.

An interesting observation has been made in regards to the differences between H_2O_2 and immunosuppressants in C6 cells. While H_2O_2 did not significantly increase ROS production, it still caused major changes of the metabolic profiles and fluxes, a result that will need to be investigated in future studies. Still, it is well documented that cancer cells in general produce more ROS than normal cells (60). Normal cells, in addition to lower ROS levels, could be better equipped to deal with oxidative stress because they can better regulate expression of enzymes that scavenge oxidants. This has been shown to be a likely mechanism for selective cancer cell killing by phenylethyl isothiocyanate, that has a chemopreventive and cancer cell selective cytotoxic activity (61).

In summary, our study on rat brain slices and primary astrocytes confirmed our hypothesis that SRL and RAD modulate CsA-induced ROS formation and subsequently CsA's effect on cell metabolism. Our results demonstrated and confirmed: (A) CsA inhibits the mitochondrial Krebs cycle and high-energy phosphate metabolism and, for compensation purposes, activates anaerobic glycolysis. (B) CsA and the ROS-inducer H_2O_2 show very similar negative effects on mitochondrial Krebs cycle and oxidative phosphorylation, thus suggesting that ROS play a key role in the negative effects of CsA. (C). While CsA primarily inhibited mitochondrial Krebs cycle, SRL inhibited anaerobic glycolysis. In CsA+SRL combination, both energy producing pathways were inhibited and the negative effects of CsA on cell energy metabolism enhanced. (D) In contrast, RAD decreased cyclosporine-induced ROS and its negative effects on mitochondrial metabolism.

Effects of immunosuppressants in brain slices and isolated astrocytes were comparable, confirming and expanding previously published results (12,32). In both models, the extent of ROS formation was associated with the extent of metabolic changes and H_2O_2 was found to cause similar metabolic changes. Both findings support our hypothesis.

The C6-glioma cell line showed a metabolic profile different from primary astrocytes and brain slices. In the controls this could likely be due to the malignant origin of the C6-glioma cell line. In the treatment groups the differences might have been due to the anti-proliferative effects of mTOR inhibitors SRL and RAD. The effects observed in C6 cells were: (A) CsA reduced the energy balance including inhibition of the Krebs cycle. (B) SRL and RAD inhibited glycolysis and the Krebs cycle metabolism while producing the highest amount of ROS. (C) The combination of CsA with SRL or RAD showed little or no additive effect with metabolism patterns similar to SRL or RAD alone.

Overall, our results suggest that SRL enhances CsA-induced ROS formation and negative metabolic effects in brain cells, while RAD seems to antagonize the CsA effects. In contrast to SRL, RAD seems to have selective negative effects on the C6-glioma cell line in terms of ROS formation and changes of cell metabolism, while having only little effect on normal rat brain tissue or astrocytes.

LIST OF ABBREVIATIONS

ATP	Adenosine Triphosphate
ADP	Adenosine Diphosphate
CsA	Cyclosporine
DCFH-DA	2', 7'-Dichlorofluorescin Diacetate
DMEM	Dulbecco's Modified Eagle's Medium
EDTA	Ethylenediaminetetraacetic Acid
FCS	Fetal Calf Serum
GABA	γ-Amino Butyric Acid
MS	Mass Spectrometry
NAA	N-Acetyl-Aspartate
NAD^+	Nicotineamide Adenine Dinucleotide (oxidized form)
NADH	Nicotineamide Adenine Dinucleotide (reduced form)
NFAT	Nuclear Factor of Activated T-cells

NMR	Nuclear Magnetic Resonance
NTP	Nucleoside Triphosphate
NDP	Nucleoside Diphosphate
PCA	Perchloric Acid
PCr	Phosphocreatine
P_I	Inorganic Phosphate
RAD	Everolimus
ROS	Reactive Oxygen Species
SRL	Sirolimus
TCA	Tricarboxylic Acid
TSP	(Trimethylsilyl) Propionic-2,2,3,3-Acid

Acknowledgments

This work was supported by the German Research Foundation (Deutsche Forschungsgemeinschaft, DFG) grant SE 985/1-1 and 985/1-2, by Novartis Pharma AG, Basel, Switzerland, and by NIH grant R01 DK065094.

REFERENCES

1. Kahan BD. Immunosuppressive therapy. Curr Opin Immunol 1992;4:553–560. [PubMed: 1418718]
2. Borel JF, Baumann G, Chapman I, Donatsch P, Fahr A, Mueller EA, Vigouret JM. In vivo pharmacological effects of ciclosporin and some analogues. Adv Pharmacol 1996;35:115–246. [PubMed: 8920206]
3. Aramburu J, Rao A, Klee CB. Calcineurin: from structure to function. Curr Top Cell Regul 2000;36:237–295. [PubMed: 10842755]
4. Serkova NJ, Christians U, Benet LZ. Biochemical mechanisms of cyclosporine neurotoxicity. Mol Interv 2004;4:97–107. [PubMed: 15087483]
5. Atkinson K, Biggs J, Darveniza P, Boland J, Concannon A, Dodds A. Cyclosporine-associated central-nervous-system toxicity after allogeneic bone-marrow transplantation. N Engl J Med 1984;310:527. [PubMed: 6363932]
6. Adams DH, Ponsford S, Gunson B, Boon A, Honigsberger L, Williams A, Buckels J, Elias E, McMaster P. Neurological complications following liver transplantation. Lancet 1987;1:949–951. [PubMed: 2882342]
7. Gijtenbeek JM, van den Bent MJ, Vecht CJ. Cyclosporine neurotoxicity: a review. J Neurol 1999;246:339–346. [PubMed: 10399863]
8. Hauben M. Cyclosporine neurotoxicity. Pharmacotherapy 1996;16:576–583. [PubMed: 8840363]
9. Crompton M, Barksby E, Johnson N, Capano M. Mitochondrial intermembrane junctional complexes and their involvement in cell death. Biochimie 2002;84:143–152. [PubMed: 12022945]
10. Serkova N, Litt L, James TL, Sadee W, Leibfritz D, Benet LZ, Christians U. Evaluation of individual and combined neurotoxicity of the immunosuppressants cyclosporine and sirolimus by in vitro multinuclear NMR spectroscopy. J Pharmacol Exp Ther 1999;289:800–806. [PubMed: 10215655]
11. Serkova N, Donohoe P, Gottschalk S, Hainz C, Niemann CU, Bickler PE, Litt L, Benet LZ, Leibfritz D, Christians U. Comparison of the effects of cyclosporin a on the metabolism of perfused rat brain slices during normoxia and hypoxia. J Cereb Blood Flow Metab 2002;22:342–352. [PubMed: 11891440]
12. Serkova N, Jacobsen W, Niemann CU, Litt L, Benet LZ, Leibfritz D, Christians U. Sirolimus, but not the structurally related RAD (everolimus), enhances the negative effects of cyclosporine on mitochondrial metabolism in the rat brain. Br J Pharmacol 2001;133:875–885. [PubMed: 11454661]

13. Wolf A, Trendelenburg CF, Diez-Fernandez C, Prieto P, Houy S, Trommer WE, Cordier A. Cyclosporine A-induced oxidative stress in rat hepatocytes. J Pharmacol Exp Ther 1997;280:1328–1334. [PubMed: 9067320]
14. Andres D, Sanz N, Zaragoza A, Alvarez AM, Cascales M. Changes in antioxidant defence systems induced by cyclosporine A in cultures of hepatocytes from 2- and 12-month-old rats. Biochem Pharmacol 2000;59:1091–1100. [PubMed: 10704938]
15. Serkova N, Christians U. Transplantation: toxicokinetics and mechanisms of toxicity of cyclosporine and macrolides. Curr Opin Investig Drugs 2003;4:1287–1296.
16. Morath C, Arns W, Schwenger V, Mehrabi A, Fonouni H, Schmidt J, Zeier M. Sirolimus in renal transplantation. Nephrol Dial Transplant 2007;22 pviii61–viii65.
17. Augustine JJ, Hricik DE. Experience with everolimus. Transplant Proc 2004;36:500S–503S. [PubMed: 15041396]
18. Serkova NJ, Christians U. Biomarkers for toxicodynamic monitoring of immunosuppressants: NMR-based quantitative metabonomics of the blood. Ther Drug Monit 2005;27:733–737. [PubMed: 16404806]
19. Kahan BD. Efficacy of sirolimus compared with azathioprine for reduction of acute renal allograft rejection: a randomised multicentre study. The Rapamune US Study Group. Lancet 2000;356:194–202. [PubMed: 10963197]
20. Kahan BD, Kramer WG. Median effect analysis of efficacy versus adverse effects of immunosuppressants. Clin Pharmacol Ther 2001;70:74–81. [PubMed: 11452247]
21. Serkova N, Litt L, Leibfritz D, Hausen B, Morris RE, James TL, Benet LZ, Christians U. The novel immunosuppressant SDZ-RAD protects rat brain slices from cyclosporine-induced reduction of high-energy phosphates. Br J Pharmacol 2000;129:485–492. [PubMed: 10711346]
22. Gordon GR, Choi HB, Rungta RL, Ellis-Davies GC, MacVicar BA. Brain metabolism dictates the polarity of astrocyte control over arterioles. Nature 2008;456:745–749. [PubMed: 18971930]
23. Rouach N, Koulakoff A, Abudara V, Willecke K, Giaume C. Astroglial metabolic networks sustain hippocampal synaptic transmission. Science 2008;322:1551–1555. [PubMed: 19056987]
24. Goya L, Feng PT, Aliabadi S, Timiras PS. Effect of growth factors on the in vitro growth and differentiation of early and late passage C6 glioma cells. Int J Dev Neurosci 1996;14:409–417. [PubMed: 8884374]
25. Vernadakis A, Kentroti S, Brodie C, Mangoura D, Sakellaridis N. C-6 glioma cells of early passage have progenitor properties in culture. Adv Exp Med Biol 1991;296:181–195. [PubMed: 1685850]
26. Easton JB, Houghton PJ. mTOR and cancer therapy. Oncogene 2006;25:6436–6446. [PubMed: 17041628]
27. Nicholson JK, Wilson ID. Opinion: understanding 'global' systems biology: metabonomics and the continuum of metabolism. Nat Rev Drug Discov 2003;2:668–676. [PubMed: 12904817]
28. Nicholson JK, Lindon JC, Holmes E. 'Metabonomics': understanding the metabolic responses of living systems to pathophysiological stimuli via multivariate statistical analysis of biological NMR spectroscopic data. Xenobiotica 1999;29:1181–1189. [PubMed: 10598751]
29. Nicholson JK, Lindon JC. Systems biology: Metabonomics. Nature 2008;455:1054–1056. [PubMed: 18948945]
30. Coen M, Holmes E, Lindon JC, Nicholson JK. NMR-based metabolic profiling and metabonomic approaches to problems in molecular toxicology. Chem Res Toxicol 2008;21:9–27. [PubMed: 18171018]
31. Booher J, Sensenbrenner M. Growth and cultivation of dissociated neurons and glial cells from embryonic chick, rat and human brain in flask cultures. Neurobiology 1972;2:97–105. [PubMed: 4572654]
32. Christians U, Gottschalk S, Miljus J, Hainz C, Benet LZ, Leibfritz D, Serkova N. Alterations in glucose metabolism by cyclosporine in rat brain slices link to oxidative stress: interactions with mTOR inhibitors. Br J Pharmacol 2004;143:388–396. [PubMed: 15339861]
33. Bass DA, Parce JW, Dechatelet LR, Szejda P, Seeds MC, Thomas M. Flow cytometric studies of oxidative product formation by neutrophils: a graded response to membrane stimulation. J Immunol 1983;130:1910–1917. [PubMed: 6833755]

34. Klawitter J, Kominsky DJ, Brown JL, Klawitter J, Christians U, Leibfritz D, Melo JV, Eckhardt SG, Serkova NJ. Metabolic characteristics of imatinib resistance in chronic myeloid leukaemia cells. Br J Pharmacol 2009;158:588–600. [PubMed: 19663881]
35. Kominsky DJ, Klawitter J, Brown JL, Boros LG, Melo JV, Eckhardt SG, Serkova NJ. Abnormalities in glucose uptake and metabolism in imatinib-resistant human BCR-ABL-positive cells. Clin Cancer Res 2009;15:3442–3450. [PubMed: 19401345]
36. Klawitter J, Anderson N, Klawitter J, Christians U, Leibfritz D, Eckhardt SG, Serkova NJ. Time-dependent effects of imatinib in human leukaemia cells: a kinetic NMR-profiling study. Br J Cancer 2009;100:923–931. [PubMed: 19259085]
37. Zwingmann C, Leibfritz D, Hazell AS. Energy metabolism in astrocytes and neurons treated with manganese: relation among cell-specific energy failure, glucose metabolism, and intercellular trafficking using multinuclear NMR-spectroscopic analysis. J Cereb Blood Flow Metab 2003;23:756–771. [PubMed: 12796724]
38. Zwingmann C, Chatauret N, Leibfritz D, Butterworth RF. Selective increase of brain lactate synthesis in experimental acute liver failure: results of a [H-C] nuclear magnetic resonance study. Hepatology 2003;37:420–428. [PubMed: 12540793]
39. Goa J. A micro biuret method for protein determination; determination of total protein in cerebrospinal fluid. Scand J Clin Lab Invest 1953;5:218–222. [PubMed: 13135413]
40. Beal MF, Brouillet E, Jenkins B, Henshaw R, Rosen B, Hyman BT. Age-dependent striatal excitotoxic lesions produced by the endogenous mitochondrial inhibitor malonate. J Neurochem 1993;61:1147–1150. [PubMed: 7689641]
41. Simonian NA, Coyle JT. Oxidative stress in neurodegenerative diseases. Annu Rev Pharmacol Toxicol 1996;36:83–106. [PubMed: 8725383]
42. Gummert JF, Ikonen T, Morris RE. Newer immunosuppressive drugs: a review. J Am Soc Nephrol 1999;10:1366–1380. [PubMed: 10361877]
43. Halliwell B. Reactive oxygen species and the central nervous system. J Neurochem 1992;59:1609–1623. [PubMed: 1402908]
44. Miller BL. A review of chemical issues in 1H NMR spectroscopy: N-acetyl-L-aspartate, creatine and choline. NMR Biomed 1991;4:47–52. [PubMed: 1650241]
45. Sonnewald U, Therrien G, Butterworth RF. Portacaval anastomosis results in altered neuron--astrocytic metabolic trafficking of amino acids: evidence from 13C-NMR studies. J Neurochem 1996;67:1711–1717. [PubMed: 8858957]
46. Tsai G, Coyle JT. N-acetylaspartate in neuropsychiatric disorders. Prog Neurobiol 1995;46:531–540. [PubMed: 8532851]
47. Brooks WM, Stidley CA, Petropoulos H, Jung RE, Weers DC, Friedman SD, Barlow MA, Sibbitt WL Jr, Yeo RA. Metabolic and cognitive response to human traumatic brain injury: a quantitative proton magnetic resonance study. J Neurotrauma 2000;17:629–640. [PubMed: 10972240]
48. Shuto H, Kataoka Y, Fujisaki K, Nakao T, Sueyasu M, Miura I, Watanabe Y, Fujiwara M, Oishi R. Inhibition of GABA system involved in cyclosporine-induced convulsions. Life Sci 1999;65:879–887. [PubMed: 10465348]
49. Tominaga K, Yamauchi A, Shuto H, Niizeki M, Makino K, Oishi R, Kataoka Y. Ovariectomy aggravates convulsions and hippocampal gamma-aminobutyric acid inhibition induced by cyclosporin A in rats. Eur J Pharmacol 2001;430:243–249. [PubMed: 11711037]
50. Genova ML, Pich MM, Bernacchia A, Bianchi C, Biondi A, Bovina C, Falasca AI, Formiggini G, Castelli GP, Lenaz G. The mitochondrial production of reactive oxygen species in relation to aging and pathology. Ann N Y Acad Sci 2004;1011:86–100. [PubMed: 15126287]
51. Serkova N, Christians U, Flogel U, Pfeuffer J, Leibfritz D. Assessment of the mechanism of astrocyte swelling induced by the macrolide immunosuppressant sirolimus using multinuclear nuclear magnetic resonance spectroscopy. Chem Res Toxicol 1997;10:1359–1363. [PubMed: 9437526]
52. Plas DR, Thompson CB. Akt-dependent transformation: there is more to growth than just surviving. Oncogene 2005;24:7435–7442. [PubMed: 16288290]
53. Edinger AL, Linardic CM, Chiang GG, Thompson CB, Abraham RT. Differential effects of rapamycin on mammalian target of rapamycin signaling functions in mammalian cells. Cancer Res 2003;63:8451–8460. [PubMed: 14679009]

54. Serkova N, Hausen B, Berry GJ, Jacobsen W, Benet LZ, Morris RE, Christians U. Tissue distribution and clinical monitoring of the novel macrolide immunosuppressant SDZ-RAD and its metabolites in monkey lung transplant recipients: interaction with cyclosporine. J Pharmacol Exp Ther 2000;294:323–332. [PubMed: 10871329]

55. Feeney CJ, Frantseva MV, Carlen PL, Pennefather PS, Shulyakova N, Shniffer C, Mills LR. Vulnerability of glial cells to hydrogen peroxide in cultured hippocampal slices. Brain Res 2008;1198:1–15. [PubMed: 18261717]

56. Panwalkar A, Verstovsek S, Giles FJ. Mammalian target of rapamycin inhibition as therapy for hematologic malignancies. Cancer 2004;100:657–666. [PubMed: 14770419]

57. Vignot S, Faivre S, Aguirre D, Raymond E. mTOR-targeted therapy of cancer with rapamycin derivatives. Ann Oncol 2005;16:525–537. [PubMed: 15728109]

58. Hjelmeland AB, Lattimore KP, Fee BE, Shi Q, Wickman S, Keir ST, Hjelmeland MD, Batt D, Bigner DD, Friedman HS, Rich JN. The combination of novel low molecular weight inhibitors of RAF (LBT613) and target of rapamycin (RAD001) decreases glioma proliferation and invasion. Mol Cancer Ther 2007;6:2449–2457. [PubMed: 17766837]

59. Warburg O. On the origin of cancer cells. Science 1956;123:309–314. [PubMed: 13298683]

60. Szatrowski TP, Nathan CF. Production of large amounts of hydrogen peroxide by human tumor cells. Cancer Res 1991;51:794–798. [PubMed: 1846317]

61. Trachootham D, Zhou Y, Zhang H, Demizu Y, Chen Z, Pelicano H, Chiao PJ, Achanta G, Arlinghaus RB, Liu J, Huang P. Selective killing of oncogenically transformed cells through a ROS-mediated mechanism by beta-phenylethyl isothiocyanate. Cancer Cell 2006;10:241–252. [PubMed: 16959615]

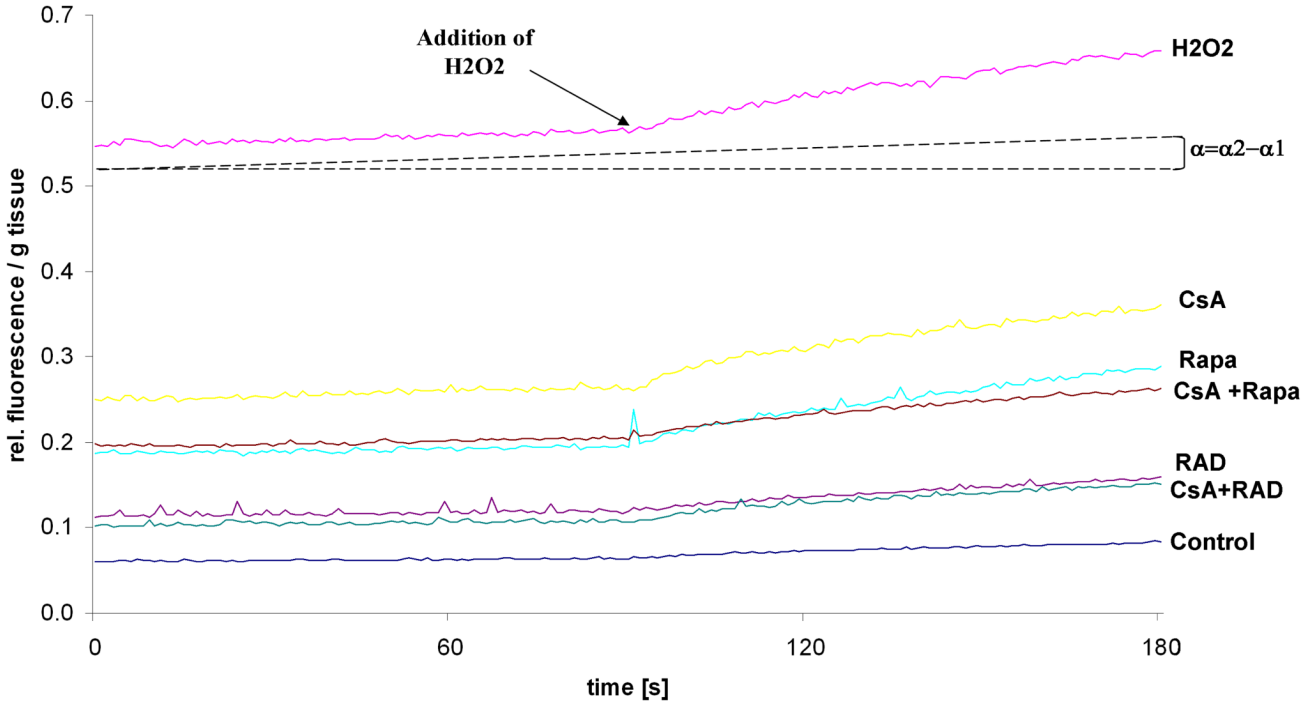

Figure 1.

Representative fluorescence recordings of brain slices treated with immunosuppressants and hydrogen peroxide (H_2O_2). Increase in fluorescence intensity, as measured by the angle α =α2-α1 (with α2: emission angle and α2>α1) correlates with the level of DCF in the cell and therefore with the ROS production. H_2O_2 was added after 90 seconds to verify loading of the cells with DCFH-dA, leading to a faster increase in fluorescence intensity.

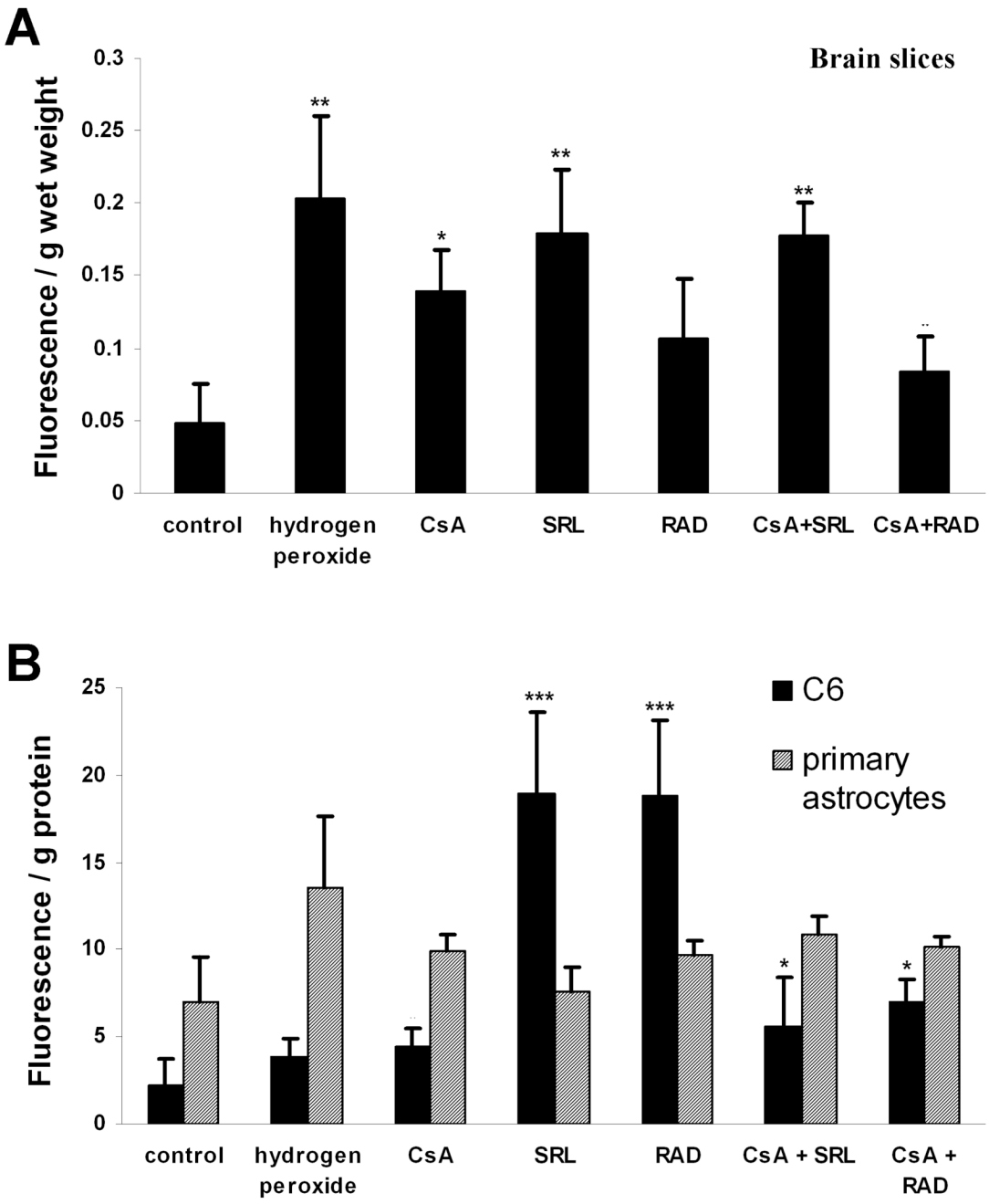

Figure 2.

(A) Formation of ROS in rat brain slices after perfusion with CsA, SRL, RAD alone or combinations of CsA with SRL or RAD (CSA: 500μg/L, SRL, RAD: 100 μg/L) for 3 hours or with 1 mM H_2O_2 for 30 minutes. One-way ANOVA confirmed significant differences among treatments ($p<0.0001$). (B) ROS-formation in primary astrocytes and C6 glioma cells after incubations with the same concentrations of the immunosuppressants for 3.5 hours or with 0.1 mM H_2O_2 for 30 minutes. All data presented as means ± standard deviations of three to six experiments. *$p< 0.05$, **$p<0.005$ versus controls. One-way ANOVA in combination with Tukey's *post-hoc* test confirmed a significant difference between SRL and RAD versus

all other treatment groups ($p<0.0001$). In the primary astrocytes model, SRL versus CsA+SRL group was significantly lower with $p<0.05$, n=5.

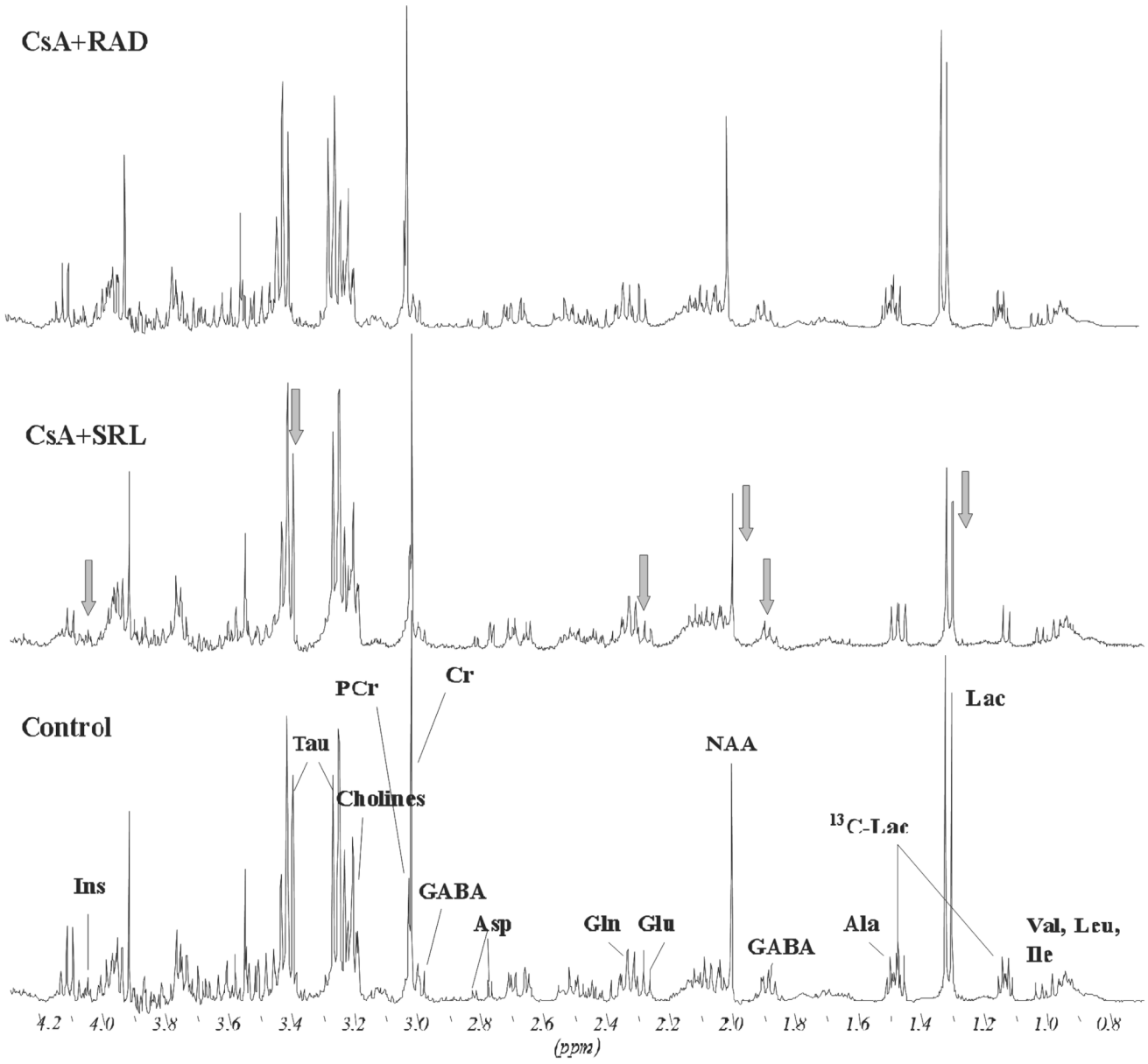

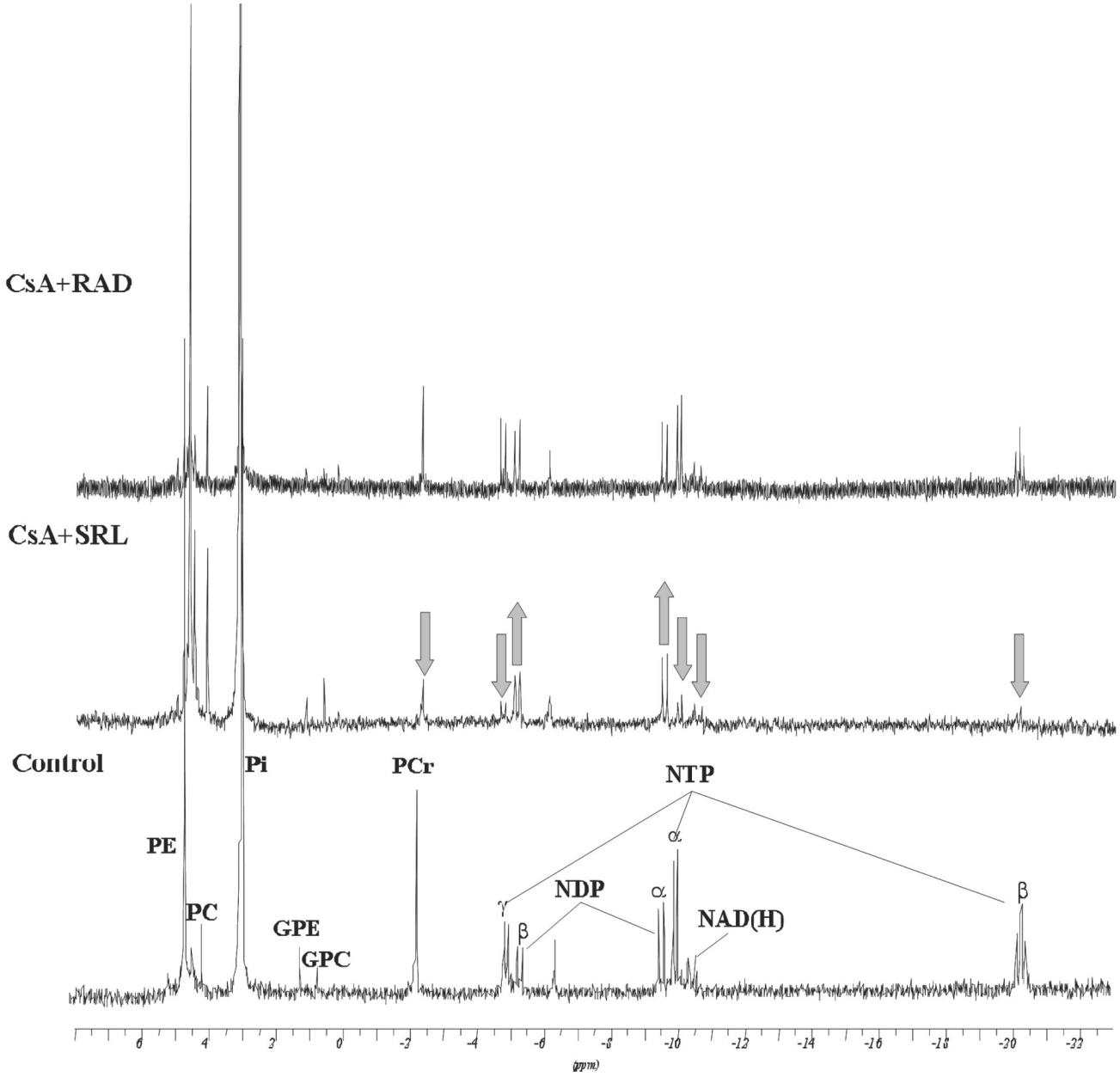

Figure 3.

Representative (A) ^{1}H–NMR and (B) ^{31}P-NMR spectra of water-soluble metabolites in rat brain slices from vehicle controls and rat brain slices exposed to the study drugs and their combinations. Brain slices were perfused with 500 μg/L CsA in combination with either 100 μg/L SRL or 100 μg/L RAD for 3 hours. Changes in metabolite concentrations are marked by arrows. Abbreviations: Ala: alanine, Asp: aspartate, Cholines: choline-containing phospholipids, Cr: creatine, GABA: γ-amino butyric acid, Gln: glutamine, Glc: glucose, Glu: glutamate, GPC: glycerophosphocholine, GPE: glycerophosphoethanolamine, Lac: lactate, myo-Ins: myo-inositol, NAA: N-acetyl-aspartate, NAD(H): nicotineamide adenine dinucleotides, NDP: nucleoside diphosphates, NTP: nucleoside triphosphates, PC: phosphocholine, PCr: phosphocreatine, PE: phosphoethanolamine, Pi: inorganic phosphate, Tau: taurine, Val/Leu/Isoleu: valine/leucine/isoleucine.

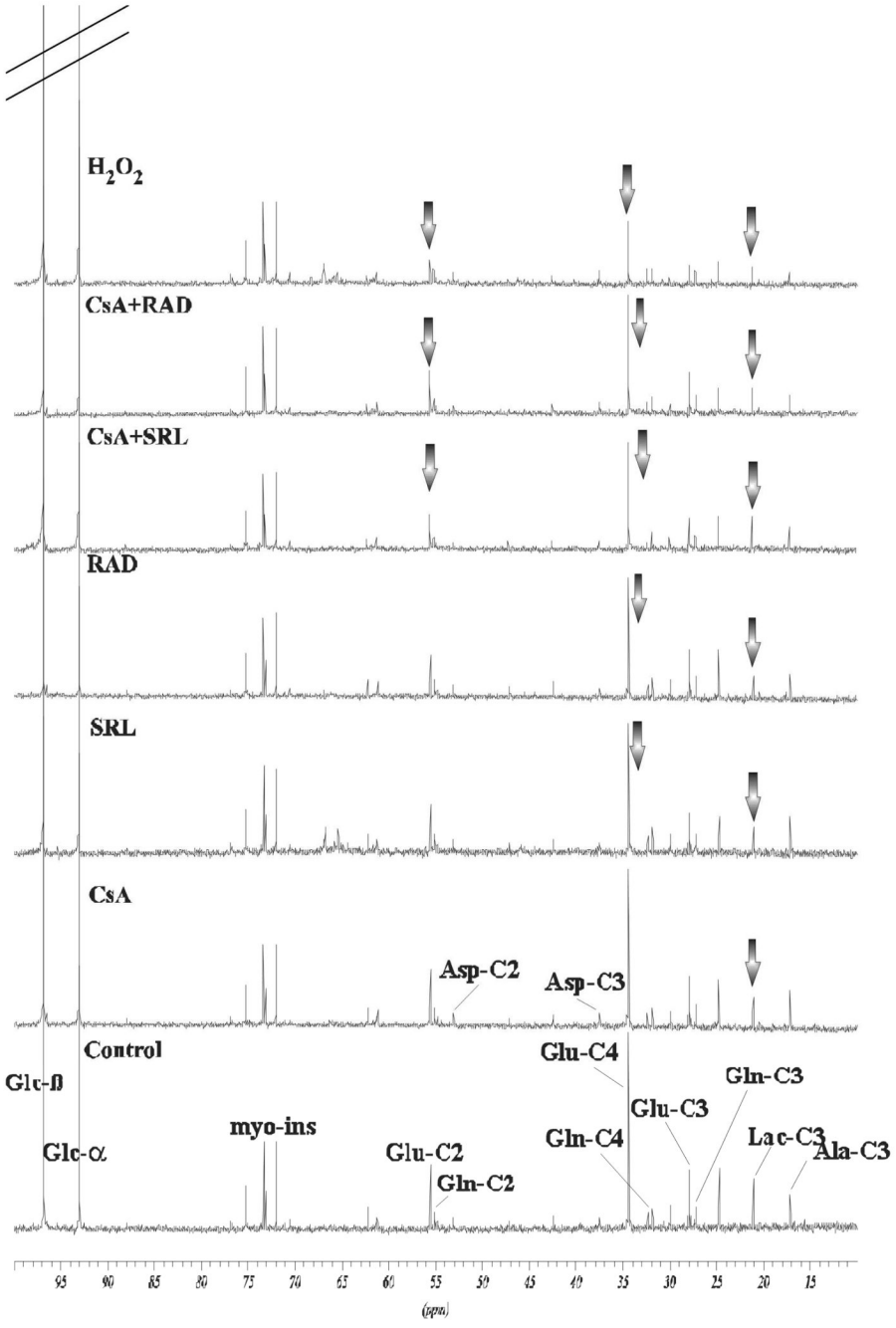

Figure 4.

Representative ^{13}C-NMR spectra of water-soluble metabolites from control and immunosuppressant-treated C6 glioma cells. The cells were incubated with 5mM [1-^{13}C] glucose for 3 hours. Treatment with immunosuppressants occurred at the same time (500 μg/L CsA, 100 μg/L SRL or 100 μg/L RAD alone or in combination with CsA for 3 hours and addition of 1 mM H_2O_2 for 30 minutes). Changes in metabolites are marked by arrows. Abbreviations: Ala: alanine, Asp: aspartate, Gln: glutamine, Glc: glucose, Glu: glutamate, Lac: lactate, myo-Ins: myo-inositol (natural abundance).

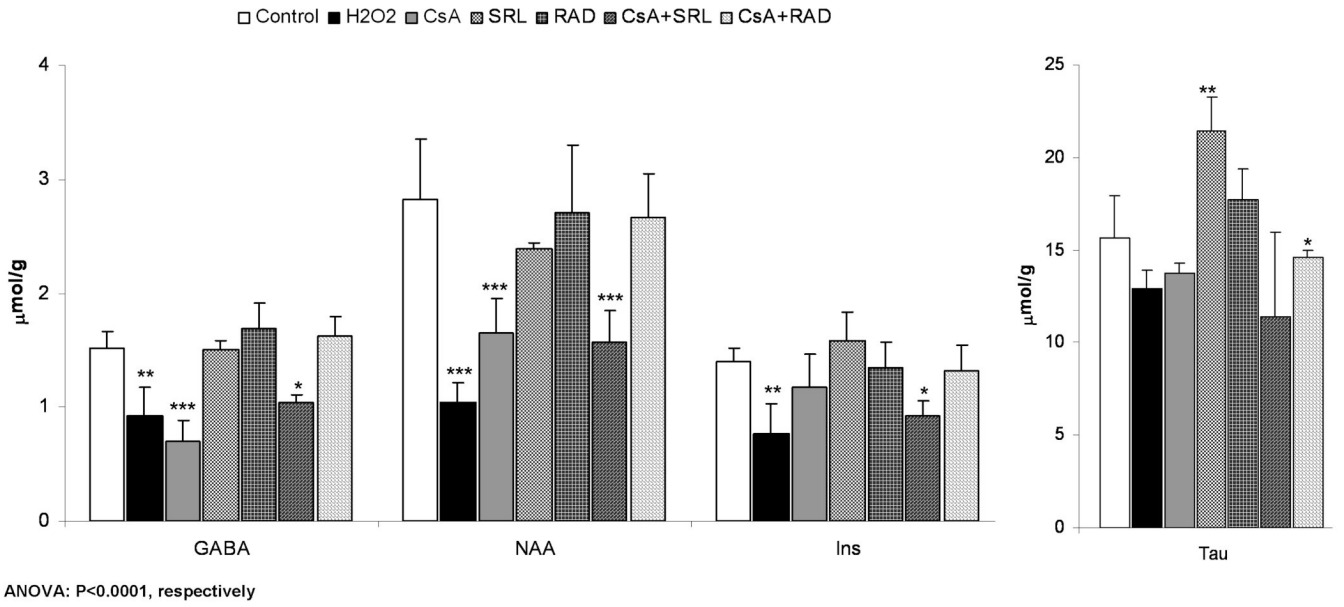

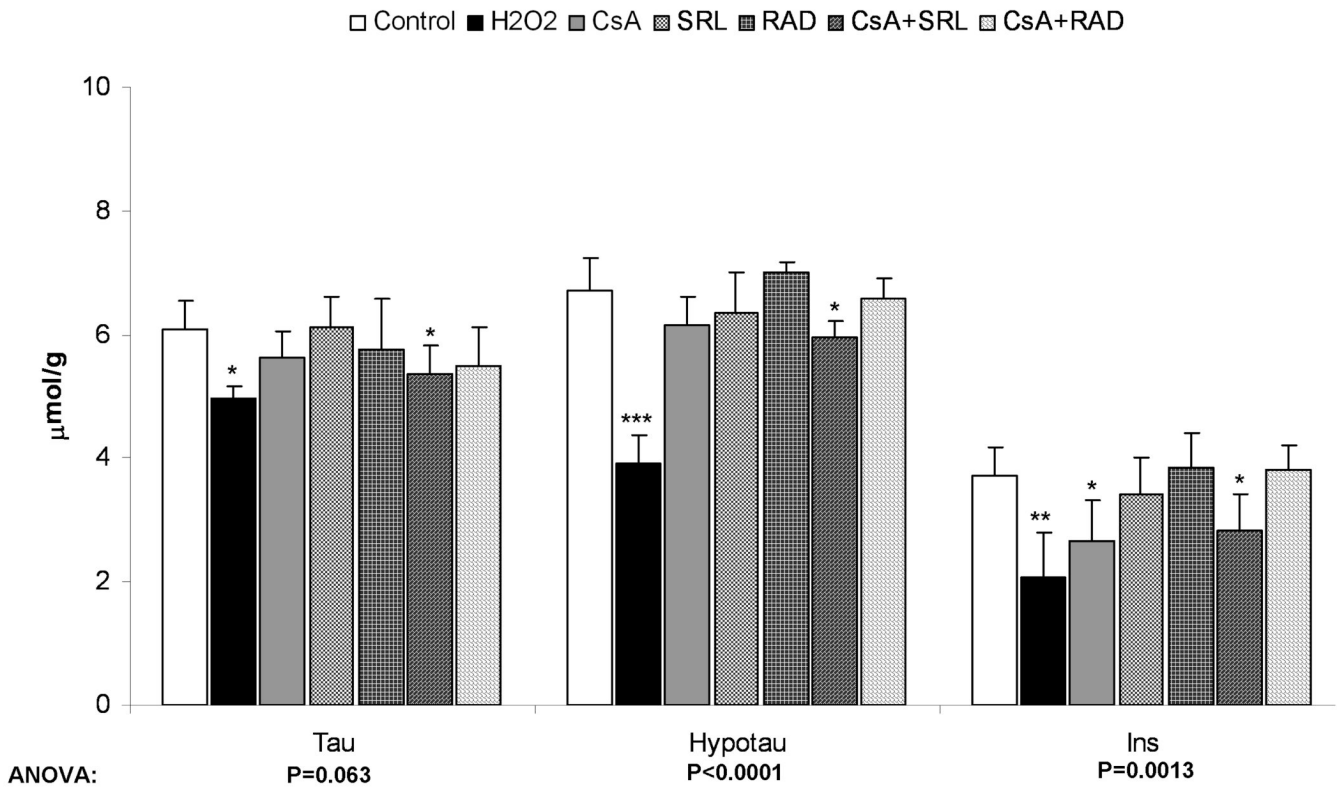

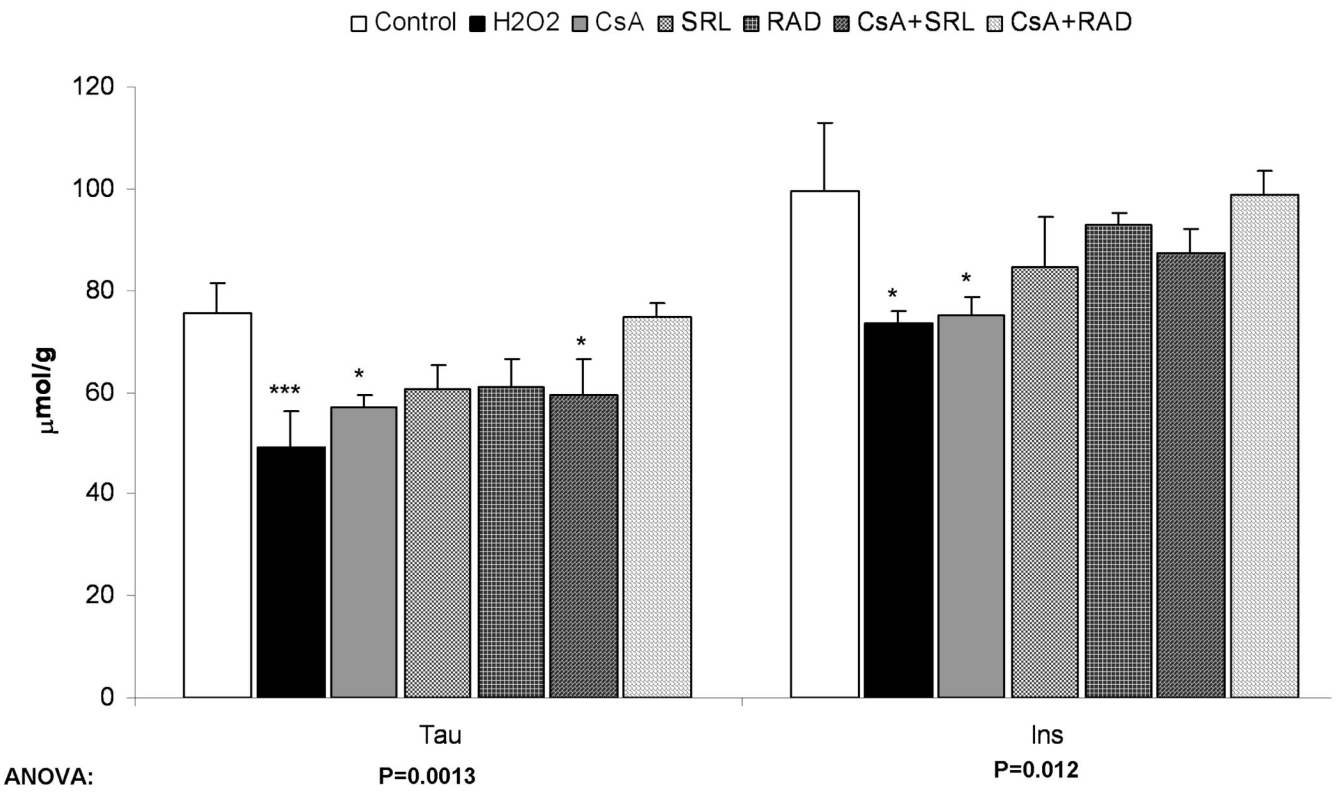

Figure 5.

Changes in volume- and osmoregulators after incubation with immunosuppressants as calculated from ^{1}H-NMR spectra. A) After perfusion of rat brain slices with immunosuppressants (500 µg/L CsA, 100 µg/L SRL or 100 µg/L RAD alone or combinations with CsA) for 3 hours or with 1 mM H_2O_2 for 30 minutes. B) After incubation of primary astrocytes with immunosuppressants (the same concentration as in rat brain slices) for 3 hours or with 0.1 mM H_2O_2 for 30 minutes. C) After incubation of C6 cells with the same concentrations of the immunosuppressants for 3 hours or with 0.1 mM H_2O_2 for 30 minutes. All values are given as µmol/g (tissue for brain slices and protein for astrocytes and C6 cells) and are means ± standard deviations of three to six experiments. One-way ANOVA with Tukey's *post-hoc* analysis was performed and the significance between groups is presented within the graphs. Significance levels compared with controls are presented: *$p<0.05$, **$p<0.005$, ***$p<0.001$.

Abbreviations: GABA: γ-aminobutyric acid, Hypotau: hypotaurine, Ins: myo-inositol, NAA: N-acetylaspartic acid, Tau: taurine.

Table 1

Comparison of the effects of immunosuppressants and H_2O_2 on the concentration of ^{13}C-labeled glucose, lactate and glutamate in perfused rat brain slices, C6 glioma cells and primary astrocytes as calculated from ^{13}C-NMR spectra of water soluble PCA-extracts.

		Control	CsA	SRL	RAD	CsA+SRL	CsA+RAD	Positive Control (H_2O_2)
C3-Lactate	**Slices**	**1602.5±169.2**	**2042.5±355.4***	**1122.3±103.4***	**1025.0±141.5****	**927.4±54.4****	**1455.0±174.6**	**847.5±227.1****
	Astrocytes	*855.0±95.7*	*1020.0±69.8**	*707.5±66.5**	*732.5±68.0*	*667.5±124.2**	*1005.0±270.9*	*600±128.8**
	C6	185.5±11.9	120.1±10.4*	67.3±21.0**	75.6±11.0***	103.3±11.4***	85.5±13.7***	34.5±13.2***
C4-Glutamate	**Slices**	**562.0±149.5**	**338.0±57.2***	**612.4±145.1**	**482.3±130.6**	**337.6±47.2***	**464.7±129.3**	**324.9±89.3***
	Astrocytes	*701.7±39.0*	*523.4±85.5**	*690.1±83.8*	*692.8±70.3*	*519.9±75.6**	*825.2±356.4*	*587.4±162.0*
	C6	1290.9±60.4	1000.9±264.9	730.1±112.0**	675.7±207.9*	752.4±189.0*	815.8±257.1**	246.9±129.9***
Glucose	**Slices**	**3164.6±315.5**	**3395.6±465.8**	**3579.9±359.1**	**2598.1±538.3**	**2640.2±226.8***	**2734.2±591.1**	**1343.7±366.6*****
	Astrocytes	*2284.7±138.9*	*2037.6±152.1**	*2133.1±207.7*	*2205.2±330.6*	*2551.5±327.1*	*2391.0±1101.3*	*1662.3±262.9**
	C6	3326.7±482.1	3493.0±775.5	5059.6±939.8*	4082.4±1146.1	4589.7±1300.5*	3738.7±782.8	2904.1±740.1

Results are presented as means ± standard deviations (n=4, *p<0.05, **p<0.005, ***p<0.001) in nmol/g cell weight. Rat brain slices, C6 glioma cells and primary astrocytes were treated with CsA (500 µg/L), SRL (100 µg/L), RAD (100 µg/L), alone or in combination for 3 hours or with H_2O_2 (0.1 mM for cells and 1 mM for brain slices) for 30 minutes. During the drug treatment 5mM [1-^{13}C]-glucose was added into the cell/brain slices incubation medium for 3 hours. **Bold: rat brain slices** *italic: primary astrocytes*, normal: C6 glioma cells.

Chem Res Toxicol. Author manuscript; available in PMC 2011 March 15.

Table 2

Effects of immunosuppressants and H_2O_2 on high energy phosphates and NAD(H) concentrations as calculated from ^{31}P-NMR of PCA extracts.

		Control	CsA	SRL	RAD	CsA+SRL	CsA+RAD	Positive Control (H_2O_2)
PCr	**Slices**	**2.75±0.51**	**2.06±0.12***	**2.01±0.20***	**3.45±0.21***	**1.06±0.33****	**2.72±0.48**	**1.36±0.22****
	Astrocytes	*2.98±0.35*	*2.18±0.45**	*2.28±0.41**	*3.01±0.19*	*1.99±0.15***	*2.64±0.31*	*0.79±0.48****
	C6	2.75±0.13	2.22±0.87	1.98±0.08**	1.93±0.20**	1.73±0.14***	1.58±0.16***	1.28±0.43*
NTP/NDP	**Slices**	**2.13±0.13**	**1.15±0.12*****	**1.34±0.32****	**1.84±0.29**	**0.45±0.05*****	**1.74±0.24**	**0.81±0.25*****
	Astrocytes	*3.47±0.31*	*2.55±0.28**	*3.23±0.71*	*3.91±0.59*	*1.81±0.21****	*3.65±1.17*	*1.11±0.17****
	C6	9.18±0.47	6.60±0.18*	5.02±0.51***	4.59±1.03**	4.09±0.66***	4.31±0.32***	4.04±0.79**
NAD(H)	**Slices**	**0.29±0.07**	**0.17±0.05***	**0.30±0.09**	**0.53±0.05****	**0.18±0.06***	**0.31±0.10**	**0.08±0.10***
	Astrocytes	*0.55±0.07*	*0.45±0.03**	*0.48±0.06*	*0.51±0.07*	*0.32±0.08***	*0.48±0.03**	*0.17±0.04****
	C6	1.62±0.18	1.12±0.30*	1.11±0.28*	0.90±0.27*	0.74±0.21**	0.67±0.21**	0.50±0.19**

Results are presented as means ± standard deviations (n=4, *p<0.05, **p<0.005, ***p<0.001) in µmol/g weight (for PCr and NAD(H); NTP/NDP ratio is unit-less). Rat brain slices, C6 glioma cells and primary astrocytes were treated with CsA (500 µg/L), SRL (100 µg/L), RAD (100 µg/L), alone or in combination for 3 hours or with H_2O_2 (0.1 mM for cells and 1 mM for brain slices) for 30 minutes. Abbreviations: NAD(H): nicotineamide adenine dinucleotide, NDP: nucleotide diphosphates, NTP: nucleotide triphosphates, PCr: phosphocreatine. **Bold: rat brain slices** *italic: primary astrocytes,* normal: C6 glioma cells.